



Investigation of the formation of defects under fast neutrons and gamma irradiation in 3C–SiC nano powder

M.N. Mirzayev^{a,b,*}, B.A. Abdurakhimov^{b,c}, E. Demir^d, A.A. Donkov^{b,e}, E. Popov^{b,e,f}, M. Yu. Tashmetov^c, I.G. Genov^{b,g}, T.T. Thabethe^g, K. Siemek^{b,h}, K. Krezhovⁱ, F. Mamedov^{b,j}, D.M. Mirzayeva^b, M.V. Bulavin^b, V.A. Turchenko^b, T.X. Thang^k, T.Z. Abdurakhmonov^l, P. Horodek^h

^a Institute of Radiation Problems, Azerbaijan National Academy of Sciences, Baku, AZ1143, Azerbaijan

^b Joint Institute for Nuclear Research, Dubna, Moscow distr., 141980, Russia

^c Institute of Nuclear Physics, Academy of Sciences of Uzbekistan, Tashkent, 100214, Uzbekistan

^d Yeditepe University, Physics Department, Istanbul, 34755, Turkey

^e Institute of Solid State Physics, Bulgarian Academy of Sciences, Sofia, 1784, Bulgaria

^f Institute for Nuclear Research and Nuclear Energy, Bulgarian Academy of Sciences, Sofia, 1784, Bulgaria

^g Institute of Electrochemistry and Energy Systems, Bulgarian Academy of Sciences, Sofia, 1113, Bulgaria

^h Department of Physics, University of Pretoria, 0028, South Africa

ⁱ Institute of Nuclear Physics, Polish Academy of Sciences, Krakow, PL-31342, Poland

^j Institute of Electronics, Bulgarian Academy of Sciences, Sofia, 1784, Bulgaria

^k Czech Technical University in Prague, CZ-11000, Prague, Czech Republic

^l Institute of Materials Sciences, Vietnam Academy of Science and Technology, 18 Hoang Quoc Viet, Cau Giay, Hanoi, Vietnam

¹ Department of Physics, National University of Uzbekistan, 100174, Tashkent, Uzbekistan

ARTICLE INFO

Keywords:

Silicon carbide
Neutron irradiation
Defect formation
Positron annihilation
Structure defects

ABSTRACT

In this work cubic phase, silicon carbide nano-powders were irradiated at the high-flux pulsed reactor IBR-2 (Dubna, Russia). The 3C–SiC powder was irradiated with neutron doses up to 10^{15} n/cm². The irradiated samples were then analyzed using X-ray diffraction, Raman spectroscopy, Positron annihilation spectroscopy, and Fourier Transform Infrared Spectroscopy. The XRD analysis showed a slight decrease in the lattice parameters with the increase in neutron fluences. The results obtained from positron annihilation measurements were compared to the theoretical calculations, to recognizing the type of structural defect in the samples. A positron lifetime component 355 ps associated with the calculated values for clusters containing of 13–21 vacancies was identified. The concentration of these defects was estimated to be in the region of 5 ppm, and was very similar to the one identified on the unirradiated sample. The results also indicate high irradiation resistivity of the 3C–SiC after irradiation.

1. Introduction

The interest in studying the irradiation effects on silicon carbide has increased significantly for various reasons [1]. For example, in the investigation of the use of SiC material in nuclear energetic systems [2]. Although so this material has acquired its position as one of the important materials in modern engineering due to its physical and mechanical properties (e.g. high hardness, high strength, low density, high thermal conductivity, high elastic modulus, excellent thermal shock resistance, superior chemical inertness, etc.), it has also become the most

competitive material in the fission reactors (for example, TRISO fuel of high-temperature gas-cooled reactors) and the preparation of composite materials for next-generation reactors [3–5]. The exceptional properties of SiC such as high neutron radiation and high-temperature resistance have made it to be highly desirable. Currently, the effects of electrons, protons, heavy ions, and neutrons on SiC have been examined and are still being studied under different irradiation environments including different irradiation temperature [6–8]. It is known that neutrons penetrate atoms because they have no charge and directly interact with the nucleus and neutrons of the material leading to considerable

* Corresponding author. Joint Institute for Nuclear Research, Dubna, Moscow Distr, 141980, Russia. Tel.: +74962164211.

E-mail address: matlab@jinr.ru (M.N. Mirzayev).



modifications in the material properties.

This paper is aimed at studying the effects of irradiation in 3C-SiC nano-powder generated by 10^{12} – 10^{15} n/cm² neutron fluences using Raman spectroscopy, Positron annihilation techniques, Fourier Transform Infrared Spectroscopy, and X-ray diffraction. To investigate the structural modifications of the samples, X-ray diffraction and Raman spectroscopy techniques were used. The Raman spectroscopy is a sensitive and non-destructive technique to characterize the damage evolution process of the materials. It allows us to analyse the chemical and structural disorder, bonding evolution, and mechanical features of crystal materials caused by radiation irradiation [9]. Raman spectroscopy has been widely used to investigate irradiation effects on a variety of materials with the inclusion of SiC [10]. Raman peaks are subject to the crystalline structure and electronic polarization of Si-C bonds that can be affected by the defects. The response of Raman spectra to defects and crystalline structure has been used as an instrument to analyse irradiation-induced displacement damage [11]. Also, the intensity of Raman peaks in the spectrum decreases with the increasing levels of lattice damage, owing to the increase in the absorption coefficient of ceramics materials [12]. The FTIR studies provide detailed information on the status of chemical bonds, energy, and frequency of bonds, optical density in materials, and the amorphous mechanism [13]. Studies show that there are three main characteristic peaks for the SiC compound; that is, the SiC-transverse optical mode (TOM), SiC-longitudinal optical mode (LOM), and Si-O stretching mode (SM). Analysis of the SiC sample with FTIR provided information regarding the mechanism of amorphization of the field kinetics of TOM and LOM peaks at room temperature under 2.3 MeV $^{28}\text{Si}^+$ and 3.0 MeV $^{84}\text{Kr}^+$ ions [14,15]. Single amorphous silicon carbide (α -SiC) irradiated with 1.4×10^{14} n/cm² fast neutrons and the dynamics of the interaction with various chemical elements have been studied in Ref. [16]. To investigate the microstructural evolution of SiC, in this study, we calculate the positron lifetime of open-volume defects like vacancy clusters with increasing sizes using quantum-mechanical electronic structures based on the density-functional theory (DFT) and its two-component extension [17]. The basic method of these calculations is the Local Density Approximation (LDA). We have made a comparison with the experimental data of the positron lifetime (PLT). The main aim of this paper is to investigate the structural changes due to defects in SiC nano-powder samples before and after neutron irradiation.

2. Materials and methods

Silicon carbide nano-powder with a purity of 99.999%, bulk density of 0.069 g/cm³, specific surface area 70–90 m²/g, and particle size to 100 nm (Sigma-Aldrich, Germany) was used in this work. The samples were enveloped with aluminium foil and then irradiated at different doses. Neutron irradiation was conducted at the IBR-2 high-flux pulsed reactor at Frank Laboratory of Neutron Physics (JINR, Dubna, Russia). The samples were irradiated at normal conditions 293.15 K and 1 atm at fluences of 4.0×10^{12} n/cm², 8.0×10^{12} n/cm², 1.3×10^{13} n/cm², 4.0×10^{14} n/cm² and 10^{15} n/cm² (neutron energy E > 0.1 MeV) [18,19]. The γ dose rate was ~ 500 Gy/h which is about 85% of the total dose. The structural characteristics of the samples were measured using the XRD EMPYREAN PANanalytical diffractometer with a CuK α source, $\lambda = 1.5406$ Å, the tube of the diffractometer with a copper anode was at U = 40 kV voltage and the current generated was I = 40 mA. The Rietveld analysis of X-ray diffraction patterns was carried out using the FullProf software package. Raman spectroscopy experiments were performed using an INTEGRA Spectra LS PNL instrument at room temperature. The Raman spectrometer SOLAR TII was excited with 633 nm Helium-Neon laser (up to 35 mW output power), the wavelength resolution was 0.03 nm. FTIR experiment measurements were performed using the Thermo Scientific™ Smart™ iTX ATR Accessory instrument. Defect identification was performed on the irradiated samples with PALS. The positron lifetime measurements were performed at the JINR (DLNP) using a

digital spectrometer APU-8702RU with detectors based on the BaF₂ scintillators [20]. Two identical samples were placed around the isotope ^{22}Na with an activity of 27 μCi enveloped into two titanium foils with a thickness 5 μm . The timing resolution was about 180 ps. The LT 9.2 program was used to analyse the sample pattern.

In the calculations, we used a Two-Component extension of DFT (TCDFT). The positron annihilation calculation was carried out using the MIKA/doppler package [21] (conventional scheme), which implements the Kohn-Sham approach based on TCDFT [22]. The calculations were done with the help of a crystal structure initially made of 864 Si and 864 C atoms filling a $6a_0 \times 6a_0 \times 6a_0$ supercell, where a_0 is the lattice constant. Also, one has to set the structure of the modeled material, as well as to give the numerical technique to model the vacancy clusters. The β -SiC with a crystal structure similar to a zinc-blend is formed at temperatures below 1700 °C [23]. One can form the β -SiC crystal lattice if we put two FCC lattices in one another. When we build the vacancy clusters, we chose those configurations, which according to the works of Wiktor [24] are either neutral or negatively charged to be suitable for positron analysis, see also Hu [25]. The biggest size of the vacancy clusters used is 4 Si atoms and 4 C atoms. Since the SiC is a semiconductor, we have used the value of 6.52 for the appropriate dielectric constant ϵ_∞ (see, for example [26], for a general overview of results for many elements in the periodic table.).

3. Results and discussion

3.1. XRD analysis

The XRD data were analyzed using the FullProf suite by applying profile matching mode followed by full profile Rietveld refinement of the structural model. In XRD refinements a Pseudo-Voigt function was chosen to generate the line shape of the diffraction peaks and a Linear Interpolation between a set of background points with refinable heights was applied for the fitting of the background. Refinements showed, the crystal structure of the initial sample has a face-centered cubic structure, the space group is an F-43 m. Lattice parameter is $a = 4.3571$ Å. We have also checked for phases of P6₃mc, P3ml, and P3m symmetry as recommended for the SiC compositions. However, in all the cases the structure refinements we obtained the cubic F-43 m. In Fig. 1, the diffraction patterns before and after irradiation at different fluences are

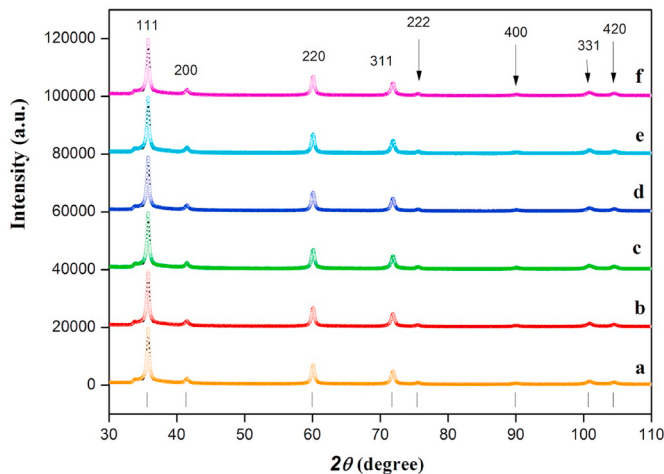


Fig. 1. Successive XRD patterns were taken for the SiC samples irradiated with different neutron irradiation fluxes and fitted by the Rietveld method. The solid lines are the experimental data, and the points are the calculated profiles. The vertical bars indicate the calculated positions of the structural diffraction peaks. The patterns are vertically shifted to improve visibility. The neutron irradiation flux values are: a) no irradiation, b) 4.0×10^{12} n/cm², c) 8.0×10^{12} n/cm², d) 1.3×10^{13} n/cm², e) 4.0×10^{14} n/cm², f) 10^{15} n/cm².

presented.

The XRD patterns show peaks only at positions characteristic of pure 3C-SiC crystallites, as indicated by the vertical bars at the bottom of Fig. 1, without the presence of other, for example, oxidized, phases. The roentgenogram results confirm the radiation resistance of SiC. The average crystallite size of the samples before and after irradiation was calculated. It shows that the size of crystallites remains constant, about ~ 25 nm. Nevertheless, it can be seen in Fig. 2, that there are small changes in the lattice parameter with the increase in the radiation fluences.

The results show, that even at small fluences at $4.0 \times 10^{12} \text{ n/cm}^2$ to $1.3 \times 10^{13} \text{ n/cm}^2$, there are small changes in the lattice parameters. That is, a small decrease from 4.3571 \AA to 4.3527 \AA is observed. At fluence 10^{15} n/cm^2 , lattice parameters further decrease to 4.3486 \AA when compared to the initial smallest radiation fluence (See Fig. 2).

3.2. Raman spectroscopy analysis

The Raman spectra were carried out between regions of 150 and 3220 cm^{-1} to investigate the irradiation damage and lattice changes of β -SiC specimens. Fig. 3 shows the Raman spectrum of the β -SiC samples before and after neutron irradiation. Four major peaks from the Raman spectra at $812\text{--}816 \text{ cm}^{-1}$, 970 cm^{-1} , 1380 cm^{-1} and $1534\text{--}1605 \text{ cm}^{-1}$ were identified. The spectrum shows vibrational modes of Si – Si bonds in the region between 150 and 600 cm^{-1} Raman shifts. In the spectrum, the strongest peak was at 816 cm^{-1} with the maximum counts of 7068 for virgin β -SiC (see the insertion in Fig. 3). The most intensive peak for all neutron irradiated β -SiC samples was determined to be at 812.8 cm^{-1} which is associated with a transverse optical (TO) phonon also known as E_1 TO phonon mode.

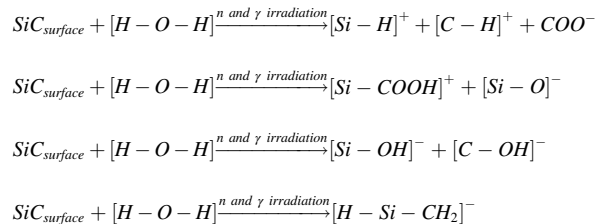
The 812.8 cm^{-1} peak for each of the different Raman spectra decreased with the increasing neutron doses up to 10^{15} n/cm^2 . The maximum count for the highest irradiation dose (10^{15} n/cm^2) was 3988. As the neutron dose increases, the intensity of the peak decreases gradually. The Relatively weak peak observed at 970 cm^{-1} is attributed to the longitudinal optical (LO) phonons [27] (also known as A_1 (LO)) of Si – C for each neutron irradiation dose as well as for the unirradiated β -SiC samples. The intensity of this peak remained almost the same, with the increasing neutron irradiation dose. However, there was a slight shift towards the left in the spectra from 967 cm^{-1} for virgin β -SiC to 957 cm^{-1} for the maximum neutron dose. It can be interpreted as an indication of the stress encountered by a certain bond between the atoms due to the neutron capturing by C and Si atoms [28]. The Raman spectra

also showed a peak with low intensity at 523 cm^{-1} for neutron-irradiated β -SiC, which is related to the TO mode of single-crystal Si [29]. It is observed with a decreasing intensity up to the 10^{15} n/cm^2 dose.

3.3. Fourier Transform Infrared Spectroscopy (FTIR) analysis

In this study, the FTIR analysis was done to study the defects before and after annealing. Fig. 4, shows the FTIR spectra before and after irradiation of the β -SiC sample at different fluences.

In the FTIR spectrum, the low frequency transverse and longitudinal patterns of $600\text{--}720 \text{ cm}^{-1}$ [Si – H] absorption bands were observed. The 780 cm^{-1} Si-C transverse optical mode (stretching vibration), the 885 cm^{-1} Si – CH₂ bands, and the 1068 cm^{-1} Si – O – Si vibrational mode frequencies observed were accompanied by a change of spectral resolution was $\Delta\nu = 4 \text{ cm}^{-1}$. In the unirradiated β -SiC sample the observation of the transverse optical mode (TOM) and longitudinal optical mode (LOM) was consistent with the results [13–15]. The increase in the irradiation dose leads to a chemical reaction with various complex mechanisms occurring on the surface of the nano β – SiC with high activity. Under the influence of the neutron fluxes, the mechanism of decomposition of water molecules takes place in a more complex phase on the surface of silicon carbide. The weak spectra in the absorption bands indicate the presence of crystalline water in the structure. It is important to have a high enough energy to remove “structural water” from the structure. “Crystalline water” also enters the coordination sphere with [Si – H]⁺, [C – H]⁺, [COO][–], [Si – COOH]⁺, [Si – OH][–], [C – OH][–], and [H – Si – CH][–] groups of Si and C atoms. A comparative analysis of the frequencies of water in the valence and deformation regions shows that the frequencies lead to the transformation of the frequencies with increasing irradiation fluences. This is also observed in the distribution of the intensity of the absorption line of the [OH] groups and the [H]⁺ molecules. The mechanism of the water molecules decomposition in the structure can be described as follows:



The irradiation is performed at room temperature in an area of 800 cm^2 , in which the ratio of neutrons and gamma rays is measured with thermoluminescent dosimeters. Low energy fast neutrons of absorbed at a neutron intensity of $1.4 \times 10^{10} \text{ n/cm}^2$ and it is 96% of the total dose. Also, the share of the total dose in the (n, γ) reaction is 85%, which is equal to $\sim 500 \text{ Gy/h}$. Based on the mechanism created by gamma and neutron irradiation together we can observe the following effects. At doses of $8.0 \times 10^{12} \text{ n/cm}^2$ and $1.3 \times 10^{13} \text{ n/cm}^2$ at a frequency of 3670 cm^{-1} , the [OH] group modes were recorded to have very low intensities. Comparative analysis with the results in the literature shows that these chemical bonds correspond to [Si – OH] modes [30]. However, at the $4.0 \times 10^{14} \text{ n/cm}^2$ irradiation dose new peaks were observed at the frequencies 2892 cm^{-1} and 2974 cm^{-1} , and the peaks characterize different interactions with Si – H and C – H. Another new weak peak is formed after irradiation with 10^{15} n/cm^2 irradiation dose and is at a frequency of 1398 cm^{-1} associated with the [H]⁺ ion. Also, the intensity of the peaks associated with neutron fluxes of the [H]⁺ ion increased due to the decomposition of the bud [H-OH] nano SiC on the surface. The disintegration of the water molecules on the SiC surface under the influence of neutron and gamma radiation is consistent with the experimental results. Also, we calculated the area of FTIR spectra of unirradiated and irradiated samples at the different neutron irradiation

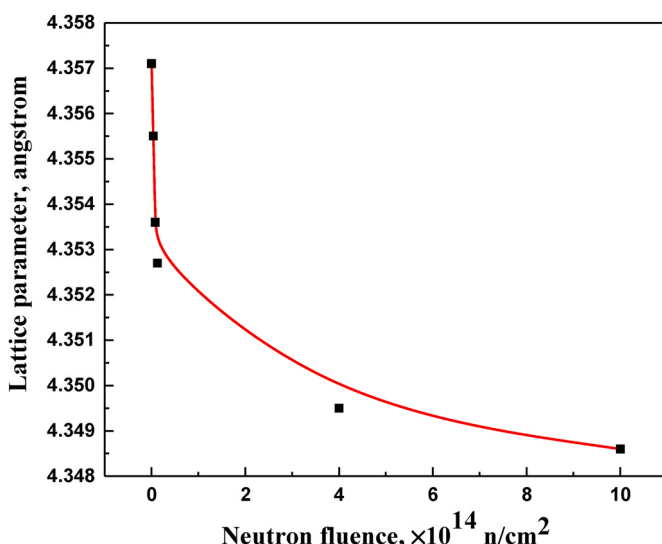


Fig. 2. The dependence of lattice parameters on the neutron fluences.

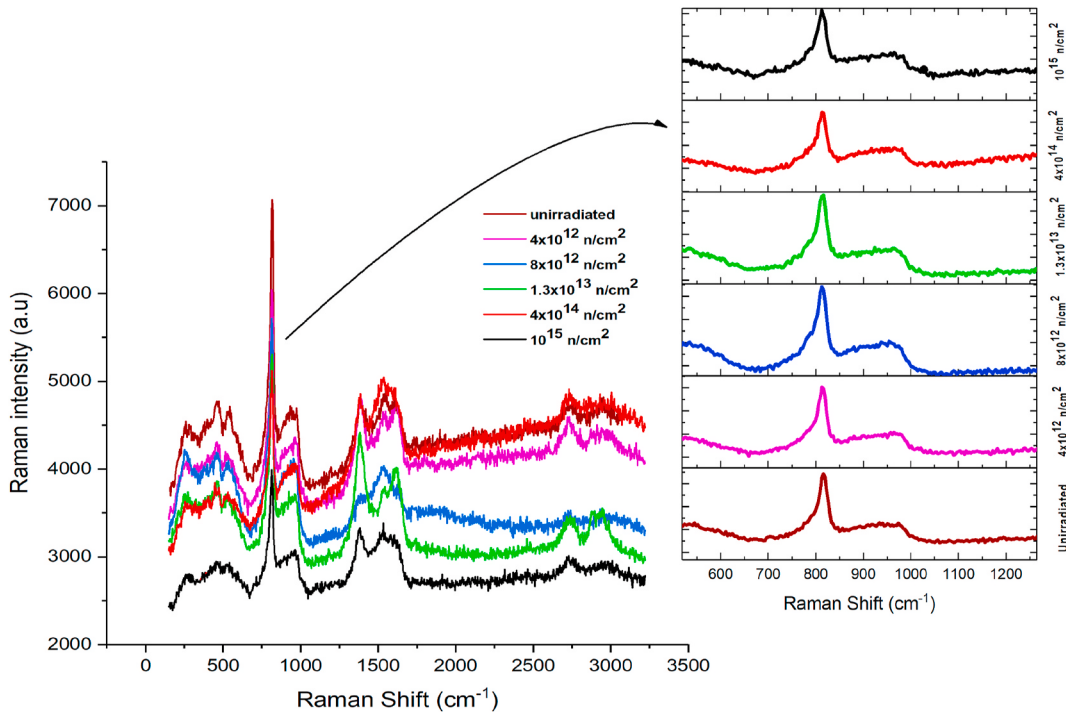


Fig. 3. Raman scattering spectra of 3C–SiC before and after irradiated with 0.1–1 MeV neutrons at neutron fluences of $4.0 \times 10^{12} \text{ n/cm}^2$, $8.0 \times 10^{12} \text{ n/cm}^2$, $1.3 \times 10^{13} \text{ n/cm}^2$, $4.0 \times 10^{14} \text{ n/cm}^2$, 10^{15} n/cm^2 , and 500 kGy at room temperature. The inset shows the expanded TO phonon region of 3C – SiC.

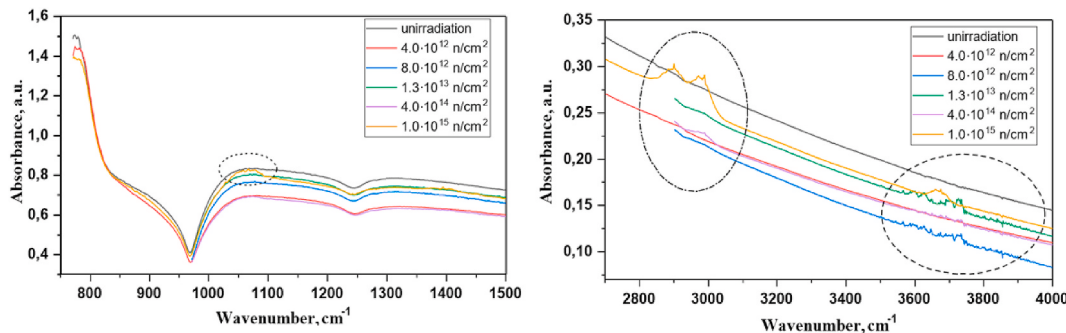


Fig. 4. Fourier transform infrared spectroscopy of nano 3CF–SiC sample at different neutron irradiation fluences.

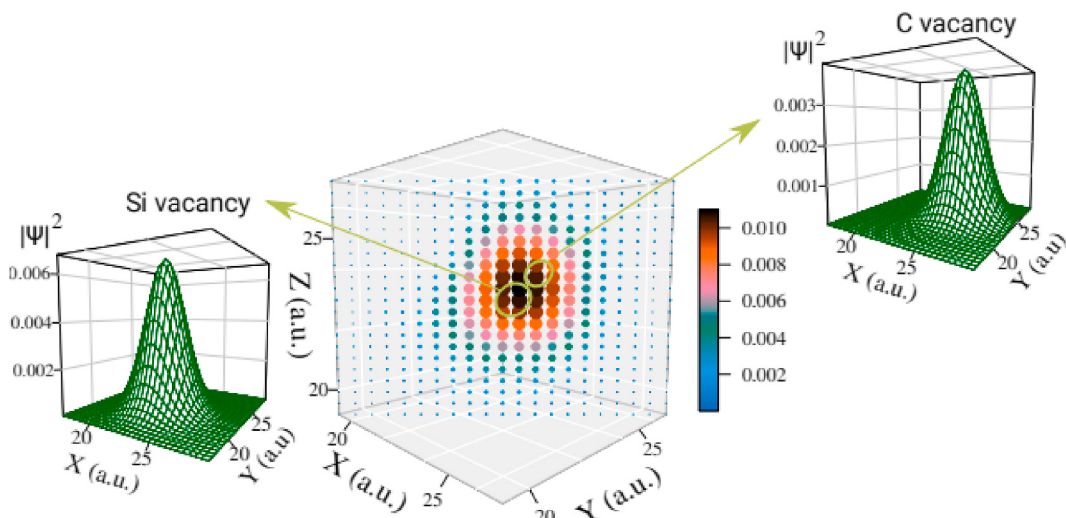


Fig. 5. Dependence of the area of the FTIR spectrum on the radiation dose for the kinetics of the amorphization mechanism.

doses (See Fig. 5).

The intensity of the irradiated samples decreased by 19.12% relative to the unirradiated sample. However, it is clear from the dependence graph that the kinetics of amorphization in the irradiated samples in the energy range 0.1–1 MeV varies as in Fig. 5. The decrease in the intensity with the increase in the irradiation dose is associated with the effective reduction in area. However, the occurrence of valence oscillations at frequencies of 2892 cm^{-1} and 2974 cm^{-1} after the irradiation dose of 10^{15} n/cm^2 increased the field variation.

3.4. Positron annihilation analysis

The numerical result for the positron lifetime (PLT) in perfect SiC lattice (with LDA) is 141 ps. For mono-vacancy, we obtained a value of 186 ps ($1V_{Si}$). This calculation was made without the relaxation, in comparison, with the relaxation the value obtained for nearest atoms for the case of $1V_{Si}$ was $\tau = 201$ ps. We considered those vacancies that are observable in PAS. For example, we eliminated the one carbon vacancy from the calculation because it was positively charged and would repulse positrons and would not be useful for the positron annihilation measurement [31]. The numerical di-vacancy ($1V_{Si} + 1V_C$) is achieved by removing one Si atom and one C atom that are next to each other along the [111] direction of the supercell. Fig. 6, presents the localized positron wave function of di-vacancies.

In Fig. 7, the graphical representation of the functional dependency of the PLT on the number of vacancies in the vacancy cluster is given.

The PLT of this di-vacancy of SiC is equal to 217 ps. In the work done by Ref. [24], the authors reported another type of di-vacancy that comes from the cluster with two removed Si atoms – $2V_{Si}$, but then one C atom moves into the vacancy position of one of the Si atoms. This complex is denoted as $1V_{Si} + 1V_C + 1C_{Si}$. The value obtained for the PLT of this complex was 221 ps and it is very close to the di-vacancy $1V_{Si} + 1V_C$. For $1V_{Si} + 2V_C$ the calculated value was $\tau = 241$ ps and for a multi-vacancy cluster ($V_{Si} + V_C$)₄ the PLT was $\tau = 320$ ps. The calculated data was compared to the experimental and other modeling results [32–34]. For completeness, we also give the PLT values that we obtained for some of the other SiC polytypes: 144.7 ps (2H – SiC), 143.4 ps (4H – SiC), 143.1

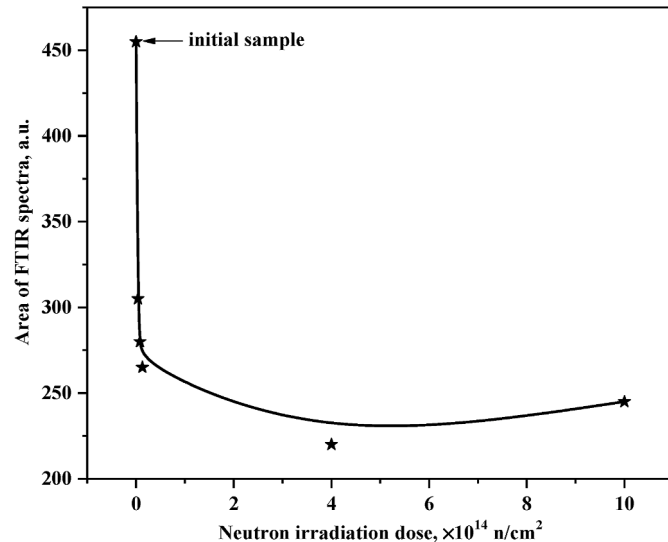


Fig. 6. The positron density, $|\psi|^2$, in the case of a di-vacancy $1V_{Si}+1V_C$ present along the diagonal [111] of the calculation cube. Here, the voxel (3-dim pixel) represented positron density for the $x = y$ cross section is shown in the middle panel, the effective positron density at the Si vacancy at the leftmost and at the C vacancy at the rightmost panel, respectively. The size and color of the voxel corresponds to the magnitude of the positron density at the voxel's position. (For interpretation of the references to color in this figure legend, the reader is referred to the Web version of this article.)

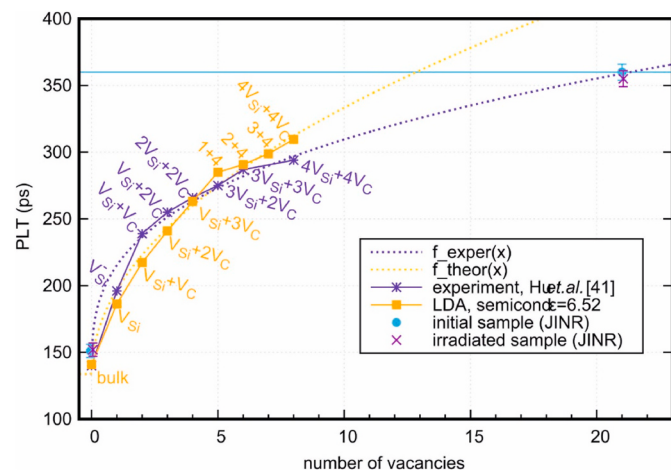


Fig. 7. PLT versus the number of vacancies in the vacancy cluster. The experimental data on the blue (dashed) line are from Ref. [25]. (For interpretation of the references to color in this figure legend, the reader is referred to the Web version of this article.)

ps (6H – SiC), and 143.3 ps (19H – SiC). Our calculations are in agreement with previous calculations with the same numerical package of the same SiC polytypes [35–37], showing the consistency of our choice for the lattice and electron orbital parameters. In recent years, the calculations for the PLT in the case of mono- and di-vacancies for 3C – SiC and 6H – SiC [24], as well extension for tetra-vacancies in 6H-SiC [25] has been performed using ABINIT [38]. Experimental measurements for PLT in neutron-irradiated 3C – SiC which have been reported in Ref. [25], were also compared to the results in Ref. [24].

The experimental PLT values were measured for the initial sample and with the neutron irradiation (in the neutron energy range 0.1–1 MeV), with the available fluence of $5.0 \times 10^{14}\text{ n/cm}^2$. Three components in the PLT spectra were obtained. The measured data are listed in Table 1. The smallest component with no irradiation was equal to 151 ps. This is close to the experimental and theoretical value for the bulk SiC ~ 141 ps, but since the material is in the form of a nano powder, the many concomitant factors, such as oxide phases and surface effects, can justify the increased PLT value in bulk. The middle component can be interpreted in two ways. If this is due to a vacancy cluster, then by extrapolation that should be drawn on Fig. 7 of the experimental data [25] it seems to correspond to 20–21 vacancies (N_{exp}). From the calculated curves, if one considers clusters of the equal number of V_{Si} and V_C , we obtain a cluster made from 13 to 14 vacancies (N_{calc}). Experimental data were extrapolated by the function: $a_1 + c_1x^{1/3}$, the calculated values were fitted to $a_2 + c_2x^{1/2}$, where x is the number of vacancies in the vacancy cluster, $a_1 = 133.6$ ps, $a_2 = 137.67$ ps, $c_1 = 81.67$ ps, $c_2 = 63.13$ ps, are the fitted coefficients. On the other hand, it can be another type of defect present. In both cases, this corresponds to a large volume void. The longest component (2.47 ± 0.053 ns) is associated with the presence of large free volumes between nano powder particles, see Fig. 8.

This can be an ortho-positronium state. Given that these volumes in real operation of the material will be limited and due to the low intensity

Table 1

Experimental results for the initial and irradiated SiC samples. The τ_3 values are related to the positron-electron annihilation in a positronium state, the values of τ_1 and τ_2 can be compared to the calculated PLT values in Fig. 7.

Sample	τ_1 (ps)	I_1 (%)	τ_2 (ps)	I_2 (%)	τ_3 (ns)	I_3 (%)
Initial	$151 \pm$	$42.43 \pm$	$360 \pm$	$56.03 \pm$	$2.47 \pm$	$1.55 \pm$
	5	0.87	6	0.87	0.053	0.53
Irradiated	$152 \pm$	$43.93 \pm$	$355 \pm$	$54.52 \pm$	$2.32 \pm$	$1.55 \pm$
	5	0.83	6	0.84	0.045	0.52

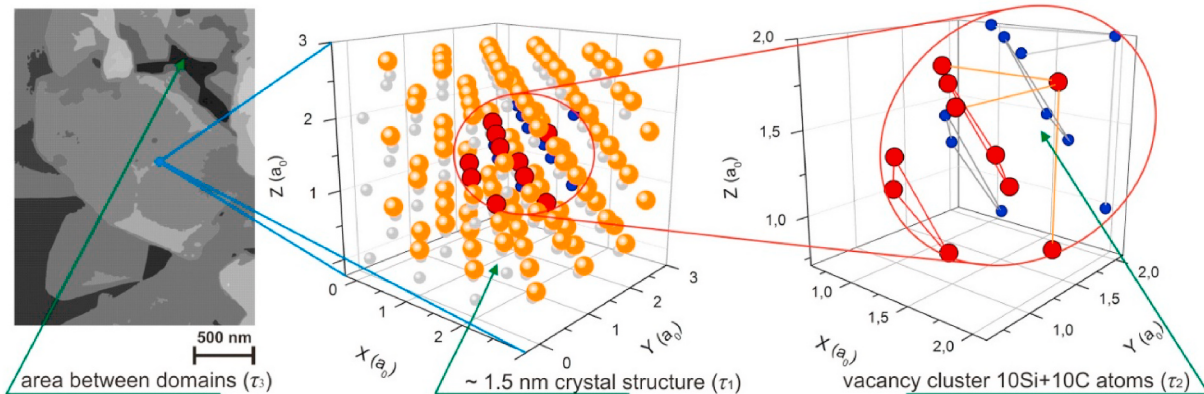


Fig. 8. Schematics of the SiC powder microstructure (left) [39], the bulk cell of SiC (center), and a typical large volume vacancy cluster (right). Illustratively, the long (ns) lived τ_3 component of the PALS originates from the area between the domains, the vacancy cluster is responsible for the τ_2 , while τ_1 comes from the bulk crystal structure.

of this component, we can neglect it. For this reason, when interpreting the results for the trapping rate we use a two-state trapping model with the help of intensity scaling of $I_b + I_1$ to 100%. For example, we use $I_{1s} = I_1/(I_1 + I_2)$ for I_1 in formula (6), with values from Table 1. For the neutron irradiated sample, the following PLT components were measured. For the bulk – τ_b (we use τ_1 to be an approximation for τ_b) we have PLT value equal to $152 \pm 5 \text{ ps}$, for the large volume defect $\tau_2 = 355 \pm 6 \text{ ps}$, and for the longest component we get $2.32 \pm 0.045 \text{ ns}$. These results show small differences from the initial sample. This suggests that the neutron irradiation in this energy range (0.1–1 MeV), with the available fluence of $5.0 \times 10^{14} \text{ ncm}^{-2}$ did not cause significant damage to the material.

With the help of the two-state trapping model [40], the data reported in Table 1 can be used to obtain the trapping rate. As mentioned earlier we use τ_1 to be an approximation for τ_b . With the relevant expressions for the annihilation (λ 's) and the trapping rates (κ 's) written as, (cf. [41, 42]):

$$\lambda_2 = 1 / \tau_2, \lambda = \lambda_b + \kappa_2, \lambda_b = 1 / \tau_b, \kappa_2 = I_2(\lambda - \lambda_2), \quad (5)$$

we can express the trapping rate in the following way:

$$\kappa_2 = \frac{I_2(\lambda_b - \lambda_2)}{1 - I_2} \quad (6)$$

By formula (6) the obtained trapping rate for the initial sample is – $\kappa_2 = 5.08 \pm 0.5 \text{ ns}^{-1}$. This value is of interest, as it is related to the vacancy concentration. For the irradiated sample, the trapping rate value is $4.67 \pm 0.5 \text{ ns}^{-1}$. The relation between the trapping rate and the vacancy defect concentration C_V is given by:

$$\kappa_2 = \mu C_V \quad (7)$$

where μ is the specific positron trapping coefficient. With the estimated value $\mu \approx 10^{15} \text{ s}^{-1}$ (e.g., Ref. [25]), and the value for the trapping rate κ_2 from Eq. (6) we obtain $C_V \sim 5 \text{ ppm}$, for the initial, and the irradiated sample. These values for the concentration are comparable to the values for the received sample in Ref. [25], and points to the cleanliness of the sample we have used.

4. Conclusions

XRD results showed a decrease of the lattice parameters of face-centered cubic nano-scale silicon carbide with the increase of neutron fluences. The results of Raman spectrometric analysis showed that as the neutron dose increases, the intensity of the Raman peaks decreases slightly. The change in the intensity of the Raman polarization was due to broken bonds and defect concentration. Moreover, there were no new

Raman peaks after the neutron irradiation up to 10^{15} n/cm^2 dose, but a shift of the peaks to lower degrees occurred. There were no significant changes in the Raman spectra of β – SiC for neutron dose between 4.0×10^{12} and 10^{15} n/cm^2 . New functional groups were observed in β – SiC samples after neutron irradiation up to 10^{15} n/cm^2 dose. With the onset of neutron irradiation, the water molecules on the surface of the materials are broken and Si and C radicals in the environment combine to form new functional groups. Functional groups reach the maximum number of fragments at the 10^{15} n/cm^2 dose, that is, the intensity of the functional groups increases with increasing neutron irradiation dose. These functional groups can be expressed as: $[\text{Si} - \text{H}]^-$, $[\text{C} - \text{H}]^-$, $[\text{COO}]^-$, $[\text{Si}-\text{COOH}]^+$, $[\text{Si} - \text{OH}]^-$, $[\text{C} - \text{OH}]^-$ and $[\text{H} - \text{Si} - \text{CH}]^-$, respectively. The lifetime component ($360 \pm 5 \text{ ps}$) corresponds to an open-volume defect. If this is a vacancy cluster, then an estimate of its size could be either $N_{\text{calc}} = 13\text{--}14$ vacancies or $N_{\text{exp}} = 20\text{--}21$ vacancies, when extrapolated from the calculated or experimental results, respectively. The neutron irradiation in the energy range 0.1–1 MeV with the available fluence of $5 \times 10^{14} \text{ ncm}^{-2}$ did not cause significant damage to the material. The values for the defect's concentration are comparable to the ones recorded for the unirradiated sample. Overall, we observe that for the bulk, in our case the Raman, the XRD, and the PALS probes, the effect of the available neutron radiation dose is similar, that is, there are only slight changes in the quantities typically measured with these techniques. On the other hand, the chemical structures that appear due to the irradiation on the surface of the SiC sample are the reason for the more pronounced changes for the quantities measured with the comparatively more surface sensitive FTIR probe.

Author contributions statements

Dr. Matlab N. Mirzayev wrote the main manuscript text, figures and reviewed the manuscript. **B.A. Abdurakhimov**: Conceptualization, Resources, Software, Investigation. **E. Demir**: Writing - review & editing, Methodology, Software. **A.A. Donkov**: Validation, Investigation. **E. Popov**: Writing - review & editing, Investigation, Funding acquisition. **M. Yu. Tashmetov**: Supervision, Resources, Methodology. **I.G. Genov**: Software, Methodology, Visualization. **T.T. Thabete**: Writing - review & editing, Conceptualization, Supervision. **K. Siemeck**: Methodology, Investigation, Visualization. **K. Krezhov**: Supervision, Validation. **F. Mamedov**: Supervision, Methodology. **D.M. Mirzayeva**: Investigation, Methodology. **M.V. Bulavin**: Investigation, Resources. **V.A. Turchenko**: Investigation, Resources. **T.X. Thang**: Software, Validation. **T.Z. Abdurakhmonov**: Methodology, Software. **P. Horodek**: Investigation, Visualization.

Declaration of competing interest

The authors declare that they have no known competing financial interests or personal relationships that could have appeared to influence the work reported in this paper.

Acknowledgement

EPP and AAD acknowledge support by the Grant of Plenipotentiary Representative of the Republic of Bulgaria at JINR.

References

- [1] T.T. Hlatshwayo, N. Mtshonisi, E.G. Njoroge, M. Mlambo, M. Msimanga, V. A. Skuratov, J.H. O'Connell, J.B. Malherbe, S.V. Motloung, Effects of Ag and Sr dual ions implanted into SiC, *Nucl. Instrum. Methods Phys. Res. Sect. B Beam Interact. Mater. Atoms* 472 (2020) 7–13, <https://doi.org/10.1016/j.nimb.2020.03.035>.
- [2] E.M. Huseynov, T.G. Naghiyev, U.S. Aliyeva, Thermal parameters investigation of neutron-irradiated nanocrystalline silicon carbide (3C-SiC) using DTA, TGA and DTG methods, *Phys. B Condens. Matter* 577 (2020) 411788, <https://doi.org/10.1016/j.physb.2019.411788>.
- [3] Y. Wu Jinxing, J. Cheng, W. Wen, Q. Wang, X. Gao, Z. Zhu, Study on effective dielectric properties of silicon carbide composites, *Phys. B Condens. Matter* 595 (2020) 412376, <https://doi.org/10.1016/j.physb.2020.412376>.
- [4] Y. Katoh, L.L. Snead, C.H. Henager, T. Nozawa, T. Hinoki, A. Ivecović, S. Novak, S. M. Gonzalez De Vicente, Current status and recent research achievements in SiC/SiC composites, *J. Nucl. Mater.* 455 (1–3) (2014) 387–397, <https://doi.org/10.1016/j.jnucmat.2014.06.003>.
- [5] I. González, A. Trejo, M. Calvino, A. Miranda, F. Salazar, E. Carvajal, M. Cruz-Irisson, Effects of surface and confinement on the optical vibrational modes and dielectric function of 3C porous silicon carbide: an ab-initio study, *Phys. B Condens. Matter* 550 (2018) 420–427, <https://doi.org/10.1016/j.physb.2018.05.024>.
- [6] V.Y. Bratus', T.T. Petrenko, S.M. Okulov, T.L. Petrenko, Positively charged carbon vacancy in three inequivalent lattice sites of 6H-SiC: combined EPR and density functional theory study, *Phys. Rev. B Condens. Matter* 71 (2005) 125202, <https://doi.org/10.1103/PhysRevB.71.125202>.
- [7] M. Tashmetov, B. Abdurakhimov, M.N. Mirzayev, T.X. Thang, The effect of electron beam on nanocrystallites size, strain and structural parameters of the silicon carbide nanopowder, *Int. J. Mod. Phys. B* 33 (20) (2019) 1950223, <https://doi.org/10.1142/S0217979219502230>.
- [8] A. Al Atem, V. Bratus, B. Canut, J. Lefevre, G. Guillot, J.M. Bluet, Combined EPR and photoluminescence study of electron and proton irradiated 3C-SiC, *Mater. Sci. Forum* 963 (2019) 301–304, [10.4028/www.scientific.net/MSF.963.301](https://doi.org/10.4028/www.scientific.net/MSF.963.301).
- [9] Silicon Carbide - Materials, Processing and Applications in Electronic Devices, 2012, <https://doi.org/10.5772/852>.
- [10] N. Chaâbane, A. Debelle, G. Sattonnay, P. Trocellier, Y. Serruys, L. Thomé, Y. Zhang, S. Sorieul, J.M. Costantini, L. Gosmain, G. Calas, J.J. Grob, L. Thomé, Study of damage in ion-irradiated α -SiC by optical spectroscopy, *J. Phys. Condens. Matter* 18 (37) (2006) 8493, <https://doi.org/10.1088/0953-8984/18/37/008>.
- [11] S. Nakashima, K. Kisoda, H. Niizuma, H. Harima, Raman scattering of disordered SiC, *Phys. B Condens. Matter* 219–220 (1996) 371–373, [https://doi.org/10.1016/0921-4526\(95\)00748-2](https://doi.org/10.1016/0921-4526(95)00748-2).
- [12] B.S. Li, C.H. Zhang, H.H. Zhang, T. Shibayama, Y.T. Yang, Study of the damage produced in 6H-SiC by He irradiation, *Vacuum* 86 (4) (2011) 452–456, <https://doi.org/10.1016/j.vacuum.2010.09.011>.
- [13] T. Kaneko, D. Nemoto, A. Horiguchi, N. Miyakawa, FTIR analysis of a-SiC:H films grown by plasma enhanced CVD, *J. Cryst. Growth* 275 (1–2) (2005) 1097–1101, <https://doi.org/10.1016/j.jcrysGro.2004.11.128>.
- [14] Y. Li, C. Chen, J.T. Li, Y. Yang, Z.M. Lin, Surface charges and optical characteristic of colloidal cubic SiC nanocrystals, *Nanoscale Res. Lett.* 6 (1) (2011) 454, <https://doi.org/10.1186/1556-276X-6-454>.
- [15] J.M. Costantini, S. Miro, O. Pluchery, FTIR study of silicon carbide amorphization by heavy ion irradiations, *J. Phys. Appl. Phys.* 50 (2017), 095301, <https://doi.org/10.1088/1361-6463/aa5614>.
- [16] J. Huran, A. Valović, P. Boháček, V.N. Shvetsov, A.P. Kobzev, S.B. Borzakov, A. Kleinová, M. Sekáčová, J. Arbet, V. Sasinková, The effect of neutron irradiation on the properties of SiC and SiC(N) layer prepared by plasma enhanced chemical vapor deposition, *Appl. Surf. Sci.* 269 (2013) 88–91, <https://doi.org/10.1016/j.apsusc.2012.10.162>.
- [17] I. Makkonen, M. Hakala, M.J. Puska, Modeling the momentum distributions of annihilating electron-positron pairs in solids, *Phys. Rev. B Condens. Matter* 73 (2006), 035103, <https://doi.org/10.1103/PhysRevB.73.035103>.
- [18] M.N. Mirzayev, Heat transfer of hexagonal boron nitride (h-BN) compound up to 1 MeV neutron energy: kinetics of the release of Wigner energy, *Radiat. Phys. Chem.* 180 (2021) 109244, <https://doi.org/10.1016/j.radphyschem.2020.109244>.
- [19] M.N. Mirzayev, High-flux neutron irradiation of boron trioxide analyzed with Raman and FTIR spectroscopy, *Int. J. Mod. Phys. B* 34 (18) (2020) 2050160, <https://doi.org/10.1142/S021797922050160X>.
- [20] P. Horodek, L.H. Khiem, K. Siemek, L.A. Tuyen, A.G. Kobets, Positron annihilation spectroscopy in material studies, *Commun. Phys.* 29 (4) (2019) 501.
- [21] I. Makkonen, M. Hakala, M.J. Puska, Modeling the momentum distributions of annihilating electron-positron pairs in solids, *Phys. Rev. B* 73 (2006), 035103, <https://doi.org/10.1103/PhysRevB.73.035103>.
- [22] E. Boronski, R.M. Nieminen, Electron-positron density-functional theory, *Phys. Rev. B* 34 (1986) 3820, <https://doi.org/10.1103/PhysRevB.34.3820>.
- [23] G. Magnani, S. Galvagno, G. Sico, S. Portofino, C. Freda, E. Burresi, Sintering and mechanical properties of β -SiC powder obtained from waste tires, *J. Adv. Ceram.* 5 (1) (2016) 40–46, <https://doi.org/10.1007/s40145-015-0170-0>.
- [24] J. Wiktor, X. Kerbiriou, G. Jomard, S. Esnouf, M.F. Barthe, M. Bertolus, Positron annihilation spectroscopy investigation of vacancy clusters in silicon carbide: combining experiments and electronic structure calculations, *Phys. Rev. B* 89 (2014) 155203, <https://doi.org/10.1103/PhysRevB.89.155203>.
- [25] X. Hu, T. Koyanagi, Y. Katoh, B.D. Wirth, Positron annihilation spectroscopy investigation of vacancy defects in neutron-irradiated 3C-SiC, *Phys. Rev. B* 95 (2017) 104103, <https://doi.org/10.1103/PhysRevB.95.104103>.
- [26] J.M.C. Robles, E. Ogando, F. Plazaola, Positron lifetime calculation for the elements of the periodic table, *J. Phys. Condens. Matter* 19 (2007) 176222, <https://doi.org/10.1088/0953-8984/19/17/176222>.
- [27] L. Zhang, W. Jiang, C. Pan, R.C. Fadanelli, W. Ai, L. Chen, T. Wang, Raman study of amorphization in nanocrystalline 3C-SiC irradiated with C^+ and He^+ ions, *J. Raman Spectrosc.* 50 (8) (2019) 1197–1204, <https://doi.org/10.1002/jrs.5631>.
- [28] E. Wendler, T. Bierschenk, F. Felgenträger, J. Sommerfeld, W. Wesch, D. Alber, G. Bukalis, L.C. Prinsloo, N. Van Der Berg, E. Friedland, J.B. Malherbe, Damage formation and optical absorption in neutron irradiated SiC, in: Nuclear Instruments and Methods in Physics Research, Section B: Beam Interactions with Materials and Atoms, vol. 286, 2012, pp. 97–101, <https://doi.org/10.1016/j.nimb.2012.01.010>.
- [29] B. Li, H. Liu, T. Shen, L. Xu, J. Wang, F. Zhao, D. Peng, J. Li, Y. Sheng, A. Xiong, Irradiation-induced microstructure damage in He-irradiated 3C-SiC at 1000°C, *J. Eur. Ceram. Soc.* 40 (4) (2020) 1014–1022, <https://doi.org/10.1016/j.jeurceramsoc.2019.11.026>.
- [30] A.M. Rossi, T.E. Murphy, V. Reipa, Ultraviolet photoluminescence from 6H silicon carbide nanoparticles, *Appl. Phys. Lett.* 92 (2008) 253112, <https://doi.org/10.1063/1.2950084>.
- [31] L. Torpo, M. Marlo, T.E. M Staab, R.M. Nieminen, Comprehensive ab initio study of properties of monovacancies and antisites in 4H-SiC, *J. Phys. Condens. Matter* 13 (2001) 6203–6231, <https://doi.org/10.1088/0953-8984/13/28/305>.
- [32] A. Kawasuso, M. Yoshikawa, H. Itoh, T. Chiba, T. Higuchi, K. Betsuyaku, F. Redmann, R. Krause-Rehberg, Electron-positron momentum distributions associated with isolated silicon vacancies in 3C-SiC, *Phys. Rev. B* 72 (2005) 45204, <https://doi.org/10.1103/PhysRevB.72.045204>.
- [33] G. Brauer, W. Anwand, P. Coleman, A. Knights, Positron studies of defects in ion-implanted SiC, *Phys. Rev. B* 54 (1996) 3084, <https://doi.org/10.1103/PhysRevB.54.3084>.
- [34] G. Brauer, W. Anwand, E.M. Nicht, J. Kuriplach, M. Sob, N. Wagner, P.G. Coleman, M.J. Puska, T. Korhonen, Evaluation of some basic positron-related characteristics of SiC, *Phys. Rev. B* 54 (1996) 2512, <https://doi.org/10.1103/PhysRevB.54.2512>.
- [35] R. Avavikko, *Positron Lifetime Spectroscopy : Digital Spectrometer and Experiments in SiC*, Ph.D. thesis, Helsinki University of Technology, 2006.
- [36] C.R. Ashman, G. Pennington, Nitrogen adsorption phases on the 4H-SiC(0001) Si-face, *Surf. Sci.* 602 (2008) 3617, <https://doi.org/10.1016/j.susc.2008.10.013>.
- [37] A. Polity, S. Huth, M. Lausmann, Defect characterization in electron-irradiated 6H-SiC by positron annihilation, *Phys. Rev. B* 59 (1999) 10603, <https://doi.org/10.1103/PhysRevB.59.10603>.
- [38] J. Wiktor, G. Jomard, M. Torrent, Two-component density functional theory within the projector augmented-wave approach: accurate and self-consistent computations of positron lifetimes and momentum distributions, *Phys. Rev. B* 92 (2015) 125113, <https://doi.org/10.1103/PhysRevB.92.125113>.
- [39] C. Wu, T. Gao, J. Nie, X. Liu, Synthesis and growth of 6H-SiC and 3C-SiC in an Al–Si–C system at 820 °C: effect of the reaction path on the SiC polytype, *Cryst. Growth Des.* 20 (2020) 1070–1078, <https://doi.org/10.1021/acs.cgd.9b01394>.
- [40] R. Krause-Rehberg, H.S. Leipner, *Positron Annihilation in Semiconductors*, vol. XV, SpringerVerlag Berlin Heidelberg, 1999, p. 383.
- [41] M. Liu, J. Cizek, C.S.T. Chang, J. Banhart, Early stages of solute clustering in an Al-Mg-Si alloy, *Acta Mater.* 91 (2015) 355–364, <https://doi.org/10.1016/j.actamat.2015.02.019>.
- [42] D. Giebel, J. Kansy, Point defect study in $Fe_{72}Al_{28}$ alloy as a function of thermal treatment by Positron Lifetime Spectroscopy, *Mater. Sci. Forum* 666 (2011) 50–53.